Desalination and Water Treatment
www.deswater.com

doi: 10.5004/dwt.2018.23060

131 (2018) 282–290
November

Kinetic and thermodynamic studies of the adsorption of Pb(II), Cr(III) and Cu(II) onto modified bentonite

Faiza Zahaf[a,*], Reda Marouf[a], Fatima Ouadjenia[a], Jacques Schott[b]

[a]*Laboratory of Materials, Applications and Environment, Mustapha Stambouli University, B.P 763 Mamounia road, Mascara 29000, Algeria, Tel. +213 45 81 39 98, Fax +213 45 81 39 98, email: zahaf.faiza@yahoo.fr (F. Zahaf), reda_marouf@hotmail.com (R. Marouf), fatouadj2@yahoo.fr (F. Ouadjenia)*
[b]*Laboratoire Géosciences Environnement Toulouse, CNRS (UMR 5563)-OMP-Universite Paul-Sabatier, Toulouse, France, email: jacques.schott@get.obs-mip.fr*

Received 31 January 2018 ; Accepted 28 August 2018

ABSTRACT

Clays intercalated with organic molecules and/or hydroxy-metal cations, also known as inorganic–organic clays (IOCs), have attracted a great deal of attention among researchers in recent years. In the present work, cetyltrimethyl ammonium bromide (CTMAB) and hydroxy-aluminum (Al_{13}) were selected to be used as intercalants in bentonite that was originally brought from the town of Mostaganem (Algeria). The modified bentonite materials were used to adsorb three heavy metals, namely Pb(II), Cr(III) and Cu(II). Some samples of B–Al and B–CTAB were prepared and characterized using different techniques, like XRD, FTIR, and BET. The adsorption process was carried out under various operational conditions by varying the temperature, initial concentration of metal and contact time. The results obtained indicated a significant increase of the interlayer spacing after intercalation with CTAB. The BET surface area also increased. The sequence of adsorption capacity for the three metals was found to be like $Cr^{3+} > Pb^{2+} > Cu^{2+}$. The adsorption kinetics could be very well described using the pseudo-second order kinetic model. The Intra-Particle Diffusion (IPD) model for sorption was also investigated and compared to other models; it was used to identify the sorption mechanism. Several thermodynamic studies found out that the adsorption process is endothermic and spontaneous in nature.

Keywords: Bentonite; Modified clay; Heavy metals; Adsorption kinetics

1. Introduction

Clays are hydrous aluminosilicates; they are defined as those minerals that make up the colloid fraction (<2 μm) of soils, sediments, and rocks [1]. Clays play an important role in the environment; they act as natural scavengers of pollutants by taking up cations and anions either through ion exchange or adsorption or both. Bentonite is a 2:1 type clay mineral. Its unit layer structure consists of one $A1^{3+}$ octahedral sheet placed between two Si^{4+} tetrahedral sheets. The cations present in the interfoliar space can be exchanged and replaced by hydroxy-metal polycations or surfactants, which can be fixed onto the layers irreversibly, leading to 'pillared' materials [2–5]. The objective of pillaring clay is to obtain microporous materials with a rigid structure and with an important interlayer spacing [6]. Polyhydroxy aluminum cation intercalation in clay consists of the insertion of "Al_{13}", referred to as the Keggin molecule [$AlO_4Al_{12}(OH)_{24}(H_2O)_{12}$], between the layers [7]. In this paper, the synthesis of organoclays was realized through ion exchange between bentonite and cethyltrimethylammonium bromide (CTAB). This type of surfactant can change the surface properties from hydrophilic to hydrophobic [8].

With the rapid increase in global industrial activities, heavy metal pollution has become serious [9]. Heavy metals may come from various industrial sources such as electroplating, metal finishing, textile, storage batteries, lead smelting, mining, plating, ceramic and glass industries. Lead, chromium and copper are common contaminants of industrial wastewaters. Because they pose serious environmental problems and are dangerous to human health, considerable

*Corresponding author.

1944-3994 / 1944-3986 © 2018 Desalination Publications. All rights reserved.

attention has been paid to methods for their removal from industrial wastewaters [10,11]. Various treatment processes, such as chemical precipitation, ion exchange, membrane separation and activated carbon adsorption, have recently been developed to remove heavy metals from wastewaters [12]. Unfortunately, some of these methods may sometimes be ineffective, extremely expensive or generating a secondary pollution. It is therefore crucial to develop an efficient, low cost and economic method for that purpose. Some natural materials, such as zeolites, chitosans and clays, are being considered as alternative low-cost adsorbents [13]. In order to enhance the heavy metal adsorbing capacity of the natural adsorbents, many attempts, such as the structural modification of clays, have been made [14–19].

The bentonite used in this study was brought from the town of Mostaganem (Northwestern Algeria). Several analytical techniques, such as XRD, BET, and chemical composition, were used to identify the samples before and after intercalation. The sorbent samples were prepared using purified raw bentonite; this was followed by the insertion step. The adsorption properties of Pb^{2+}, Cu^{2+} and Cr^{3+} were also evaluated at a variable temperature.

2. Materials and methods

2.1. Materials

The bentonite used in this study was purchased from the M'zila bentonitic clay deposit (Mostaganem, NW Algeria). This material is produced by BENTAL Company. The raw bentonite is generally intended for exportation, but doped bentonite is used essentially for drilling. In the present study, the raw bentonite was purified first and then sieved at 80 µm. For the purification of bentonite, 20 g of raw clay are dispersed in a test tube containing 1 litre of distilled water under stirring for 20 min at room temperature, and then the clay suspension is left to rest for one night. The recovered supernatant is filtered, dried at 80ºC overnight, crushed, sieved and stored in a desiccator. 10 g of the bentonite obtained is immersed in a solution containing 500 ml HCl (0.5 N) under magnetic stirring at room temperature for 4 h to remove the carbonates $(CO_3)^{2-}$. The clay is then filtered and washed with distilled water until the chloride ions tested with silver nitrate $AgNO_3$ disappear. The clay is then dried, ground, sieved and stored in a desiccators. 10 g of clay obtained are put in 500 ml of hydrogen peroxide (H_2O_2) overnight, and the recovered clay is filtered by centrifugation and then washed with distilled water.

2.2. Metal solution

1000 ppm stock solutions of Pb(II), Cu(II) and Cr(III) were prepared by dissolving 1.59 g of $Pb(NO_3)_2$ (Prolabo), 2.68 g of $CuCl_2{\cdot}2H_2O$ (Fluka) and 5.12 g of $CrCl_3{\cdot}6H_2O$ (Prolabo), in 1 L of deionized Milli-Q water, respectively.

2.3. Preparation of hydroxy-aluminum and Cetyltrimethylammonium bromide (CTAB)

The pillaring solution of hydroxy-aluminum cations ($[Al_{13}O_4(OH)_{24}(H_2O)_{12}]^{7+}$) was prepared by adding NaOH solution (0.2 mol/L) to $AlCl_3$ solution (0.2 mol/L) under vigorous stirring at 60ºC, until ratio molar $OH^-/Al^{3+} = 2$ was reached [20]. The solution was aged at room temperature for three days before using.

Cetyltrimethylammonium bromide (CTAB) with chemical formula of $C_{19}H_{42}NBr$ and molecular weight 364.45 g/mol was supplied by Merck, Germany. An amount of 1 g of bentonite was first dispersed in 100 mL of distilled water for 24 h at room temperature under vigorous agitation. Then, a desired amount of CTAB (175 mg), which is 1.0 times CEC of bentonite, was slowly added at 60ºC. After 4 h of stirring, the organoclay was filtered, washed with distilled water several times, and dried at 80ºC in oven.

2.4. Preparation of Al-intercalated bentonite and CTAB-intercalated bentonites

In order to obtain the Al-pillared bentonite, the pillaring solution of hydroxy-aluminum cations ($[Al_{13}O_4(OH)_{24}(H_2O)_{12}]^{7+}$) was added to bentonite. Then, the mixture was kept under continuous stirring for 4 h, at the temperature of 70ºC, at the ratio of 50 mmol oligomeric cations to one gram of bentonite [21]. The synthesis of CTAB-modified bentonite was performed following the procedure reported in several previous works [22]. The solids obtained were designated as B-Al and B-CTAB.

2.5. Adsorption experiments

The reagents used in the present study, i.e. Pb $(NO_3)_2$, $CrCl_3$, $CuCl_2$, NaOH, and HNO_3, were all of extra pure analytical grades. To start the experiments, a volume of 20 ml of a heavy metal solution was placed in a 100 ml bottle. The initial metal ion concentrations used in the experiments ranged from 30 to 200 mg/L. 0.1 g of material was added to each solution. It is worth noting that a high pH can cause precipitation of some metals, and low pH can cause little or no adsorption at all. In order to have a high adsorption capacity and to avoid the precipitation of cations, it is necessary to adjust the suspensions to pH = 5.5 ± 0.2, using solutions of NaOH or HNO_3 [23,24]. The mixtures obtained were agitated at a speed of 200 rpm, at the temperature of 22ºC, for 3 h.

The specific amount of solute adsorbed was calculated using the following mass balance Eq. (1):

$$q_e = \frac{C_0 - C_e}{m} * V \quad (1)$$

where q_e is the adsorption capacity of the adsorbent at equilibrium (mg g^{-1}); C_0 and C_e are the initial and equilibrium concentrations of solute, respectively (mg L^{-1}); V is the volume of the aqueous solution (L) and m is the mass of adsorbent used (g).

2.6. Characterization of bentonite

The chemical composition of natural bentonite (NB) was performed with X-fluorescence XRF 9900, Thermo Scientific™ ARL™ instrument. The X-ray analyses were

performed using INEL CPS 120 diffractometer using cobalt Kα radiation (λ = 0.178 nm), operating at 40 kV and 25 mA, and supplied with a fixed slit. The specific surface area of solid was measured at 77 K, by adsorption of nitrogen via a Quantachrome instrument, at the temperature of –196°C. The final concentrations of metals were determined using the flame atomic absorption spectrometer (FAAS, Perkin Elmer).

3. Results and discussions

3.1. Characterization of raw and modified bentonite

The physicochemical properties of raw bentonite are given in Table 1. The chemical composition results indicated the presence of oxides of some chemical elements such as silicon, aluminum, calcium, magnesium, iron, sodium and titanium. The percentage of loss ignition was found equal to 1.55%. The silica, alumina, and lime are the major oxides in the sample, and the trace elements such as iron, magnesium, sodium, titanium, sulfate, and phosphor oxides are considered as impurities. The CEC of the B–Al and B–CTAB were measured as 150 and 168 meq/100 g respectively.

The cation exchange capacity (CEC) of the modified bentonite was higher than for raw bentonite because both anions introduced additional adsorption sites when adsorbed onto the bentonite surface.

X-ray diffraction patterns of the samples are illustrated in Fig. 1. X-ray diffractogram of the BN showed a characteristic d001 peak of montmorillonite at 2θ = 8.07° (d = 1.27 nm) and two other peaks corresponding to the illite and the kaolinite at 2θ equal 10° and 13.75°, respectively. The hydroxy-aluminum polycations exchange increases the d001 value to 1.43 nm, but the peak was much less intense compared to that of natural bentonite, this is in agreement with previous results cited by Yan et al. [25]. The reduction in diffractogram of the B–Al relative to the BN was probably

Table 1
Some physicochemical properties of bentonite and modified bentonite

	B
$\%SiO_2$	64.22
$\%Al_2O_3$	11.62
%CaO	9.33
$\%Fe_2O_3$	4.88
%MgO	3.47
$\%Na_2O$	3.38
$\%TiO_2$	1.06
$\%SO_3$	0.46
$\%P_2O_5$	0.03
Loss on ignition %	1.55
pH	8.3
CEC (meq/100 g)	112
Specific surface area (m^2/g)	59.02

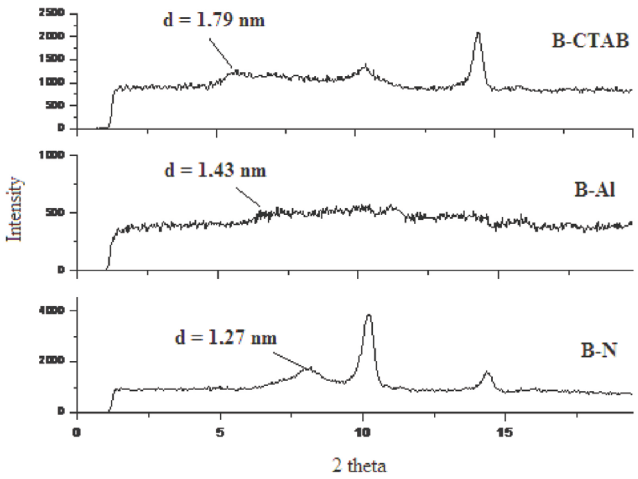

Fig. 1. XRD patterns of natural and modified bentonites.

due to the delamination of Mt layers by ions. The reduction in diffractogram might also be caused by collapsing of the Mt layers due to partial incongruent phase transition of hydroxy-Al into Fe/Al oxides and their interactions during aging and drying, as suggested by Thomas et al. [26].

The addition of surfactant causes the increasing of basal spacing of the bentonite around 18 A°, indicating location of CTA^+ ions between layers of montmorillonite. In order to further increase the basal spacing, CTA^+ concentration must be increased, because as known, the amount of added surfactant has a direct effect on the interlayer expansion of Mt. The addition of CTAB in natural bentonite increases the basal spacing more than the addition of hydroxy-aluminum. These results are in agreement with previous works in the literature [27].

Moreover, Table 1 summarizes the BET surface areas and total pore volumes for the different samples. The BET surface area of B–CTAB was found much larger than those of B–Al and BN. Besides, the specific surface areas of B–Al and B–CTAB were increased to 110 and 194.4 m^2/g, respectively. These findings are in good agreement with results previously reported by some authors [28,29]; they compared the specific area values of adsorbents based on montmorillonite modified by Al, Fe, Fe Fe/Al and that of Hexdecyl-trimethyl-ammonium bromide.

3.2. Infrared spectroscopy

The FT-IR spectra of modified bentonite (B–Al and B–CTAB) are illustrated in Fig. 2. Shows the appearance of new peaks relative to B-N which indicate the insertion of alkylamines in the interfoliary galleries of our clays. The spectrum of the B-N shows an intensive band at 1000 cm^{-1} which is attributed to the Si O in-plan stretching vibration and other bands at 520 and 470 cm^{-1} assigned to Al O Si (octahedral Al) and Si O Si bending vibrations respectively [30]. The small band at at 1620 cm^{-1} is attributed to the deformation vibrations of the O–H bond of the constitution water. The band at 3620 cm^{-1} is assigned to hydroxyl groups Al^{3+} is partially replaced by Fe^{3+} and Mg^{2+}. The band at 692 cm^{-1} confirmed presence

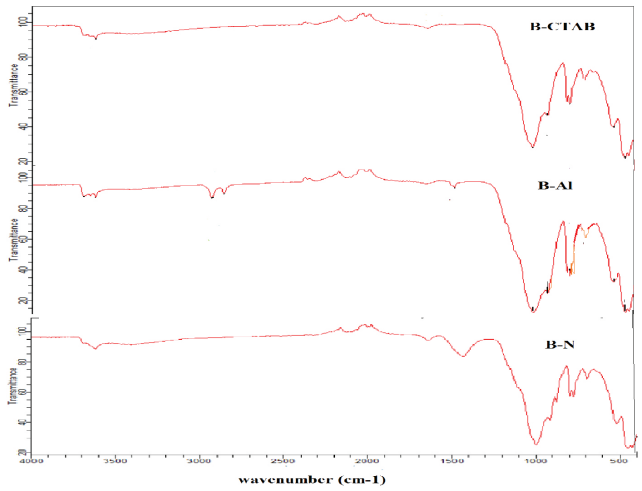

Fig. 2. Fourier transformed infrared spectra of bentonite and modified bentonite.

of quartz which coordinated to octahedral Al^{3+} cations [31]. Three peaks in the hydroxyl bending region around 920 cm^{-1} for Al_2OH, 885 cm^{-1} for AlFeOH, and 845 cm^{-1} for AlMgOH reflect that octahedral already confirmed by XRD [32]. However, the broad bands at 2928 cm^{-1}, 2852 cm^{-1} and 1465 cm^{-1} are ascribed to the C-H stretching vibration as a result of the intercalation of bentonite by Al_{13} cations and CTAB surfactant. The results indicated that CTAB and Al_{13} may be present on the surface or in the interlayer space of bentonite.

3.3. Effect of contact time

The amount of 0.1 g of modified bentonite was mixed with 20 mL of metal solution, with a concentration of 20 mg/L of Pb(II), Cr(III) and Cu(II). The suspension was mechanically agitated within the range time of 5–180 min; the supernatants were then collected for metal analysis. In the case of B–CTAB, only Pb(II) and Cu(II) were tested. The amount of metal ion adsorbed was obtained from the difference between the initial concentration and equilibrium concentration of metal ions.

The adsorption of Pb(II), Cr(III) and Cu(II) onto the two adsorbents B–Al and B–CTAB increased with time and reached equilibrium after about 60 min for B–Al and 90 min for B–CTAB (Figs. 3a, 3b). The kinetic adsorption data of Pb(II), Cr(III) and Cu(II) were determined using the pseudo-first order and pseudo-second order kinetic models [33]. Therefore:

$$Ln(q_e - q_t) = Lnq_e - K_1 t \quad (2)$$

where q_t (mg/g) is the amount of metal adsorbed at time t, K_1 (mg/(g min)) is the equilibrium rate constant of the pseudo-first order kinetic model and q_e (mg/g) is the quantity of metal adsorbed at equilibrium. The pseudo-second order equation may be written in a linear form as:

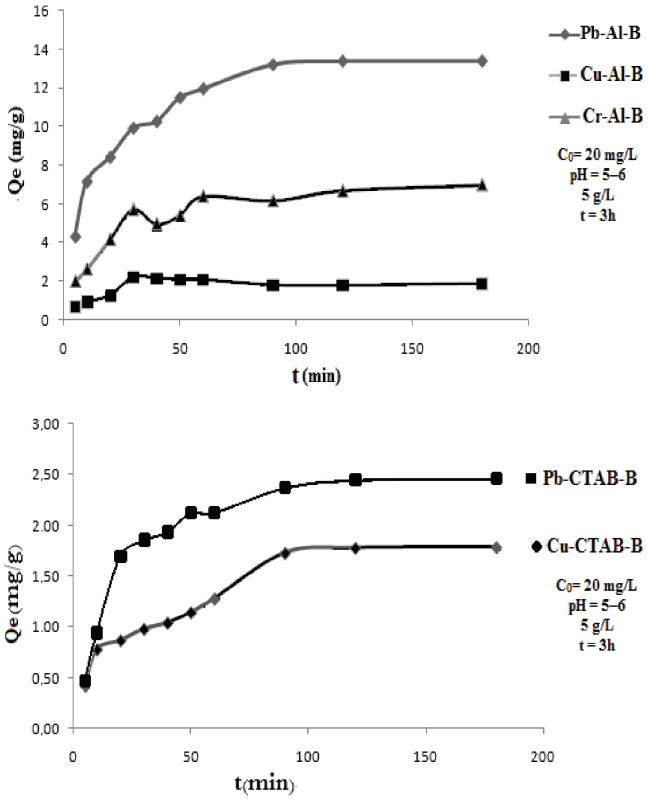

Fig. 3. (a). Effect of contact time on Pb(II), Cu(II) and Cr(III) adsorptions onto B–Al, (b). Effect of contact time on Pb(II) and Cu(II) adsorptions onto B-CTAB.

$$\frac{t}{q} = \frac{1}{K_2 q_e^2} + \frac{t}{q_e} \quad (3)$$

The parameters in these two models can be determined from the linear plots of ln $(q_e - q_t)$ versus t and t/q_t versus t, respectively. From the results presented in Table 2, one can clearly notice that the values of the correlation coefficient R^2 for the pseudo-first order model are not high for both sorbents. Furthermore, the value of q_e calculated from the pseudo-first order model is not consistent with the experiment's data. However, good correlation coefficients are obtained by fitting the experimental data to equation (3), indicating that the sorption processes of Pb(II), Cr(III) and Cu(II) follow the pseudo-second order model. At the same time, the values of q_e calculated from the pseudo-second order model for the adsorption of Pb(II), Cr(III) and Cu(II) onto B–Al and B–CTAB are consistent with the experimental q_e. One can therefore say that the sorption process of the three metals onto B–Al and B–CTAB follows the pseudo-second order model rather than the pseudo-first order model.

3.4. Adsorption isotherms

The adsorption isotherm models are significantly important because they can help to investigate the way

Table 2
Kinetics parameters for sorption of Pb^{+2}, Cr^{+3} and Cu^{2+} onto both B–Al and B–CTAB

Sorbent	Sorbate	Pseudo- first-order			Pseudo- second-order			Intra-particle diffusion	
		k_1	q_e	R^2	k_2	q_e	R^2	K_1	R^2
B–Al	Pb(II)	0.042	9.75	0.973	$9.30.\ 10^{-3}$	15.63	0.998	1.166	0.983
	Cr(III)	0.001	28.24	0.969	$2.78.10^{-3}$	7.19	0.987	1.340	0.990
	Cu(II)	Ins	Ins	Ins	$2.33.10^{-2}$	2.93	0.985	0.402	0.919
B–CTAB	Pb(II)	Ins	Ins	Ins	0.109	1.66	0.992	0.0347	0.997
	Cr(III)	Ins	Ins	Ins	0.017	2.08	0.970	0.2766	0.999

an adsorbate interacts with a sorbent. The isotherms of heavy metal adsorption onto B–Al and B–CTAB were fitted to the Langmuir, Freundlich, Temkin and The Dubinin–Radushkevich (D–R) equations models. The applicability of the isotherm model to the adsorption behaviors was investigated by estimating the correlation coefficient R^2. The Langmuir isotherm model assumes that the adsorption sites on a monolayer surface are homogeneous and equivalent, and there are no interactions between adsorbate molecules on adjacent sites [34]. The equation is expressed as follows:

$$\frac{q_e}{q_m} = \frac{K_L C_e}{1 + K_L C_e} \tag{4}$$

where q_e (mmol g^{-1}) is the adsorption capacity at equilibrium, C_e (mmol L^{-1}) is the concentration of metal ions at equilibrium, q_{max} (mmol g^{-1}) is the maximum adsorption capacity of the adsorbent, and K_L (L $mmol^{-1}$) is the Langmuir constant related to the affinity of binding sites and is also a measure of free energy of adsorption.

The Freundlich isotherm is an empirical equation that describes multilayer adsorption on an energetically heterogeneous surface [35], and is expressed as:

$$q_e = K_F C_e^{1/n} \tag{5}$$

where K_F (L $mmol^{-1}$) is the Freundlich constant related to the adsorption capacity of the adsorbent, and n is the heterogeneity factor indicating the adsorption intensity of the adsorbent.

The Temkin model accounts for indirect adsorbate–adsorbate interactions on adsorption, and predicts that the adsorption heat of all the molecules in the layer decreases linearly with coverage due to adsorbate/adsorbate interactions [36]. The Temkin isotherm model is represented as:

$$\frac{q_e}{q_{\max}} = \theta = \left(\frac{RT}{\Delta Q}\right) In\left(K_T C_e\right) \tag{6}$$

$$q_e = B_T In K_T + B_T In C_e \tag{7}$$

$$B_T = \frac{q_m R}{\Delta Q} \tag{8}$$

B_T is Temkin heat of sorption (kJ/mol), and K_T is Temkin adsorption potential (L/mg).

The Dubinin–Radushkevich (D–R) isotherm model is used to explain the adsorption character whether it is chemical or physical. The linear form of the D–R equation is written as follows [37]:

$$Inq_e = Inq_m - \beta\varepsilon^2 \tag{9}$$

where q_e and q_m are described as the amount of adsorbed at equilibrium and the maximum amount of adsorbed under the optimal conditions, respectively. The β parameter is constant with a dimension of energy, ε is the Polanyi potential and can be calculated as the following equation

$$\varepsilon = [RT \ln (1+1/C_e)] \tag{10}$$

where C_e (mol L^{-1}) is the equilibrium metal ion concentration in aqueous solution.

The adsorption isotherm constants for B–Al and B–CTAB, at various temperatures, are listed in Tables 3 and 4.

According to Figs. 4 and 5, the equilibrium concentration increases with the adsorption capacity (q_e) of B–CTAB. Indeed, this concentration increases rapidly at first, and then gradually tapers off until finally it reaches the maximum point. However, the shape of the adsorption isotherms of B–Al is different from that of B-CATB. Moreover, the adsorption capacity (q_e) of B–Al increases slowly during the whole adsorption process. This may probably be attributed to high temperature which allows cations Pb^{+2}, Cr^{+3} and Cu^{2+} to attach better to the active sites of the solid. Tables 5 and 6 summarize the constants resulting from linearization and the regression coefficients R^2. The values of R^2 for the Freundlich isotherms are both above 0.99, indicating a very good mathematical fit for both models. Moreover, the R^2 values obtained with the Temkin equation were above 0.94, indicating a good mathematical fitting to the data given by both models. Temkin equation is considered as the corrected form of Langmuir equation. It is based on Langmuir equation and introduces the influence of temperature on the adsorption capacity. It is easy to observe from Tables 3 and 4 that the calculated values of $1/n$ and K_f are greater in the case of B- CTAB than in that of B–Al, which indicates that cations Pb^{+2}, Cr^{+3} and Cu^{2+} are better adsorbed by B–CTAB than by B–Al. The result obtained from the adsorption kinetics is in good agreement with the conclusion given above. All the isotherms exhibited similar

Table 3
Constants and correlation coefficients of adsorption isotherms for the adsorption of Pb^{+2}, Cr^{+3} and Cu^{2+} onto B–Al

Model	Langmuir				Freundlich			Temkin		
Ion	T°C	q_{max} (mg/g)	K_L (L/mg)	R^2	K_F mg/g $(L/mg)^{1/n}$	$1/n$	R^2	K_0 $(L{\cdot}mg^{-1})$	ΔQ (KJ mol^{-1})	R^2
Pb^{2+}	30	27.77	0.0047	0.934	0.324	0.743	0.988	0.067	2.47	0.965
	40	31.25	0.0023	0.928	0.12	0.843	0.996	0.052	0.65	0.949
	50	8.47	0.0043	0.916	0.089	0.772	0.995	0.0055	1.63	0.937
Cu^{2+}	30	Ins	Ins	0.541	0.228	0.495	0.900	0.118	2.592	0.940
	40	Ins	Ins	0.274	0.212	0.527	0.917	0.102	2.29	0.905
	50	Ins	Ins	0.435	0.343	0.227	0.988	0.171	2.467	0.978
Cr^{3+}	30	3.72	0.016	0.963	0.111	1.498	0.960	0.094	0.139	0.973
	40	4.78	0.011	0.896	0.292	1.068	0.970	0.102	0.202	0.942
	50	4.40	0.021	0.988	0.147	1.188	0.973	0.083	0.386	0.820

Table 4
Constants and correlation coefficients of adsorption isotherms for the adsorption of Pb^{+2} and Cu^{2+} onto B–CTAB

Model	D–R				Freundlich			Temkin		
Ion	q_{max} (mg/g)	B	E	R^2	K_F mg/g $(L/mg)^{1/n}$	$1/n$	R^2	K_0 $(L{\cdot}mg^{-1})$	ΔQ (KJ mol^{-1})	R^2
Pb^{2+}	7.09	–1690	0.0172	0.824	0.015	0.77	0.999	0.035	0.46	0.937
Cu^{2+}	8.98	–1239	0.0195	0.681	0.026	0.80	0.952	0.038	0.35	0.913

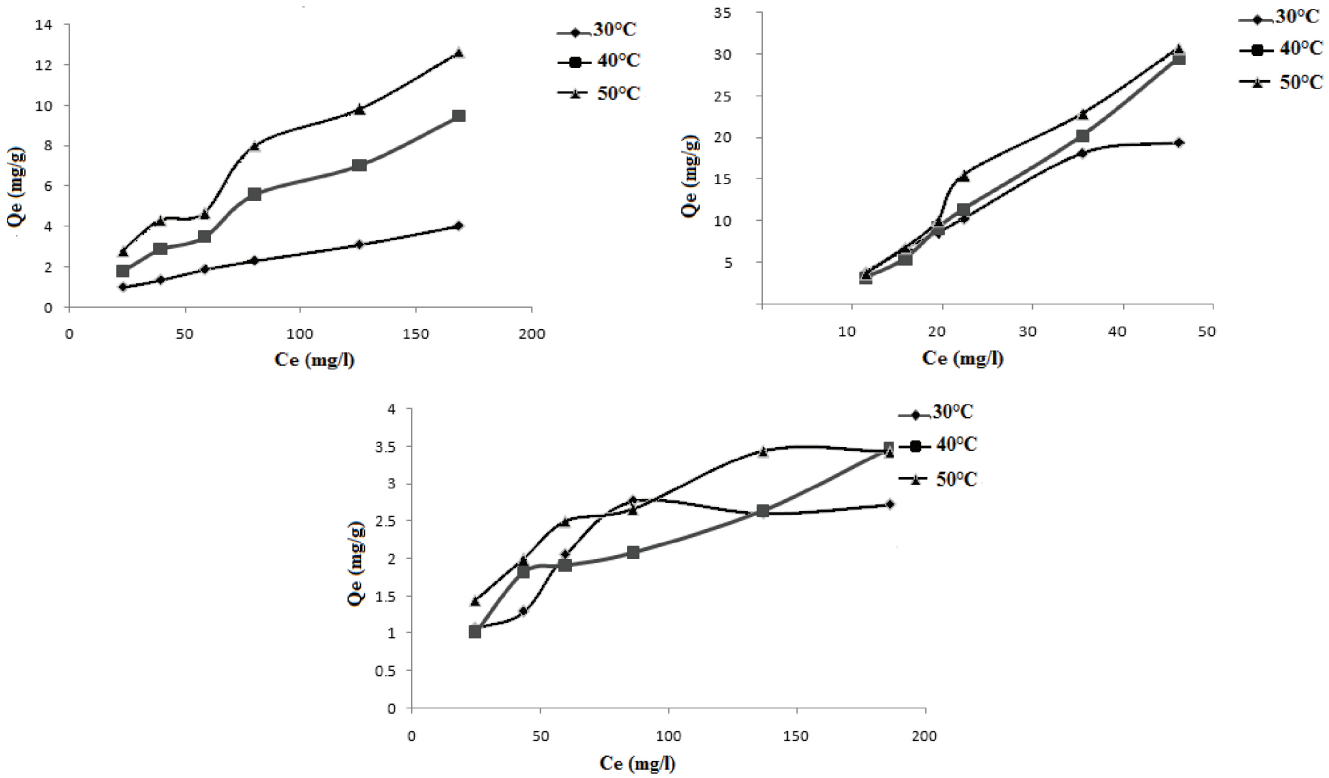

Fig. 4. (a). Effect of heavy metal concentrations for Pb^{+2} adsorption on B–Al at 30, 40 et 50°C, (b). Effect of heavy metal concentrations for Cr^{+3} adsorption on B–Al at 30, 40 et 50°C, (c). Effect of heavy metal concentrations for Cu^{+2} adsorption on B–Al at 30, 40 et 50°C.

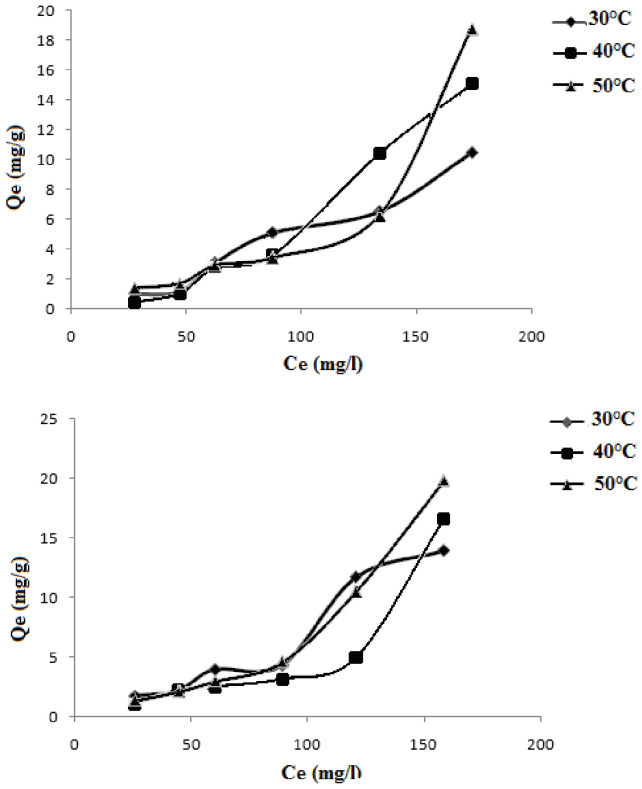

Fig. 5. (a). Effect of heavy metal concentrations for Pb^{+2} adsorption on B–CTAB at 30, 40 and 50°C, (b). Effect of heavy metal concentrations for Cu^{2+} adsorption on B–CTAB at 30, 40 and 50°C.

shapes; they are nonlinear over a wide range of aqueous equilibrium concentrations, as illustrated in Figs. 4 and 5.

3.5. Adsorption thermodynamics

The influence of temperature on Pb(II), Cr(III) and Cu(II) adsorption onto inorganic pillared bentonite was investigated at temperatures ranging from 303 to 323K, with an initial metal concentration between 30 and 150 mg/L, at pH 5–6. The thermodynamic equilibrium constants (K_d) during adsorption, i.e. the constants for metal distribution between the solid and liquid phases at equilibrium, were computed from the graph of ln (q_e/C_e) vs. $1/T$, using the method of Lyubchik et al. [38]. The thermodynamic parameters, such as the standard free energy change (ΔG^o), enthalpy change (ΔH^o), and entropy change (ΔS^o) were calculated to evaluate the feasibility and nature of the sorption process. These parameters could be obtained from the following equations [39]:

$$LnK_d = (\Delta S/R) - (\Delta H/RT) \quad (11)$$

$$\Delta G^o = \Delta H^o - T\Delta S^o \quad (12)$$

$$K_d = \frac{q_e}{C_e} \quad (13)$$

where K_d is the sorption distribution coefficient, q_e and C_e reflect the same parameters as described in the Langmuir and Freundlich equation. The ratio of activity coefficients was assumed to be uniform in the dilute range of the solutions [40]. As the concentration of the metal ion in the solution approached zero, the activity coefficient approached unity and Eq. (13) became

$$\lim_{C_e \to 0} \frac{q_e}{C_e} = K_d$$

The values of K_d are obtained by plotting (q_e/C_e) versus C_e and extrapolating to C_e = 0 [40–42]. These thermodynamic parameters are summarized in Tables 5 and 6. These tables present the thermodynamic parameters obtained for the adsorption of Cr^{+3} onto modified bentonite samples. The change in enthalpy (ΔH^o), for Pb^{+2} and Cu^{2+} metal ions, indicates that the reactions are endothermic for both adsorbents. Moreover, Kubilay et al. [43] found that the adsorption of Pb^{+2}, Cr^{+3} and Cu^{2+} ions onto modified

Table 5
Thermodynamic data for the adsorption of adsorption of Pb^{+2}, Cr^{+3} and Cu^{2+} onto B–Al

Ion	C_0 (mg/L)	R^2	ΔH (KJ·mol^{-1})	ΔS (J·mol^{-1}·K^{-1})	ΔG (KJ·mol^{-1})		
					303K	313K	323K
Pb^{2+}	30	0.999	49.00	0.178	–5.22	–6.66	–8.33
	50	0.999	2.59	0.056	–14.36	–14.45	–14.53
	70	0.975	44.57	0.166	–6.15	–7.20	–8.92
Cr^{3+}	30	0.835	15.10	0.058	–2.718	–2.844	–3.66
	50	0.833	22.92	0.082	–2.11	–2.30	–3.54
	70	0.986	19.59	0.070	–1.66	–2.40	–2.87
Cu^{2+}	30	0.981	14.44	0.022	–7.13	–7.69	–8.03
	50	0.991	29.18	0.067	–8.84	–7.77	–7.07
	70	0.608	74.44	0.004	–8.48	–8.55	–8.01

Table 6
Thermodynamic data for the adsorption of adsorption of Pb^{+2} and Cu^{2+} onto B–CTAB

Ion	C_0 (mg/L)	R^2	ΔH (J·mol^{-1}·K^{-1})	ΔS (J·mol^{-1}·K^{-1})	ΔG (KJ·mol^{-1})		
					303K	313K	323K
Pb^{2+}	50	0.994	8.17	0.044	–9.54	–9.56	–9.63
	70	0.998	6.79	0.038	–7.96	–7.99	–8.04
Cu^{+2}	70	0.961	–20.69	–0.09	–6.82	–7.95	–8.63

bentonite, at various pH values, is an endothermic process. This means that the metal uptake of these metal ions is favored at higher temperatures, since such temperatures activate the metal ions for enhancing adsorption at the coordinating sites of the minerals [44].

The values of the enthalpy change (ΔH°) in the sorption of Pb^{2+}, Cr^{3+} and Cu^{2+} metal ions on B–Al are in the ranges from 2.59 to 56.64, from 15.10 to 51.26 kJ mol^{-1} and from 10.31 to 74.44 kJ mol^{-1}, respectively. The (ΔH°) values for the adsorption of Pb^{2+} and Cu^{2+} ions onto B–CTAB were in the ranges from 6.79 to 48.67 kJ mol^{-1} and from –20.65 to 34.34 kJ mol^{-1}, respectively. The positive sign of these values indicates that this sorption process is endothermic. The standard entropy change (ΔS^0) for the adsorption process was also positive for all adsorbents.

In general, the variation of the standard entropy of the system was found higher for the adsorbents B–Al and B–CTAB than for raw bentonite. The positive sign of the entropy indicates the existence of a certain disorder at the interface between the liquid and the solid [43–45]. The negative values of ΔG° confirm the feasibility of the process and the spontaneous nature of sorption. The rise in ΔG°, as the temperature goes up, indicates that the reaction is more favorable at high temperatures. The increase in free energy change with the rise in temperature indicates that the heavy metals investigated in this study have a higher affinity for solids than for the aqueous solution when the temperature increases. Similar values of ΔH°, ΔS° and ΔG° were found for B–Al and B–CTAB, which suggests that the sorption mechanisms of Pb^{2+}, Cr^{3+} and Cu^{2+} ions on B–Al and B–CTAB are all about the same. This can be seen on the sorption isotherms previously discussed in this study.

4. Conclusion

The adsorption capacity of modified bentonites for Pb(II), Cr(III) and Cu(II) has been investigated, and the resulting experimental data showed that B–Al and B–CTAB are two efficient adsorbents of heavy metals in solutions. Lagergren first-order and second-order equations were selected to determine whether the first-order or the second-order mechanism predominates in heavy metals adsorption by modified bentonites.

The following conclusions can be drawn from this study:

- The adsorption of heavy metals on modified bentonites follows the pseudo-second order model. The adsorption rate constant increased following this sequence: Cr(III) > Pb(II) > Cu(II). The second-order kinetic model considers that the adsorption is of chemical nature (chemisorption), but according to the calculated values of enthalpy, which do not exceed 40 kJ/mol, the adsorption of heavy metals on modified bentonite is of physical nature (physisorption).
- The adsorption capacity of Cr(III), Pb(II) and Cu(II) on B–Al and B–CTAB increases as the temperature rises.
- The thermodynamic parameters of adsorption are important in understanding the adsorption mechanism. The values of the thermodynamic parameters show that the adsorption processes are spontaneous and endothermic in nature.

Symbols

NB — Natural bentonite
B-Al — Aluminum-intercalated bentonite
B-CTAB — Cetyltrimethylammonium-intercalated bentonite
D-R — Dubinin–Radushkevich
C_e — Equilibrium concentration (mg/L)
C_0 — Initial concentration (mg/L)
q_e — Amount of metal cations adsorbed (mg/g)
q_t — Amount of metal cations adsorbed at time t (mg/g)
q_0 — Maximum adsorption capacity (mg/g)
k_1 — Rate constant of pseudo-first-order (min^{-1})
k_2 — Rate constant of pseudo-second-order (g/mg min)
K_L — Langmuir adsorption constant (L/mg)
K_F — Freundlich adsorption constant (mg/g (L/mg)$^{1/n}$)
m — Mass of the adsorbent (g)
V — Volume of the solution (L)

References

[1] G. Ranga Rao, B. Gopal Mishra, A comparative UV-vis-diffuse reflectance study on the location and interaction of cerium ions in Al- and Zr-pillared montmorillonite clays, Mater. Chem. Phys., 89 (2005) 110–115.
[2] B. Gopal Mishra, G. Ranga Rao, Physicochemical and catalytic properties of Zr-pillared montmorillonite with varying pillar density, Micropor. Mesopor. Mater., 70 (2004) 43–50.
[3] M.D. Bhor, N.S. Nandurkar, M.J. Bhanushali, Ultrasound promoted selective synthesis of 1,1′-binaphthyls catalyzed by Fe impregnated pillared montmorillonite K10 in presence of TBHP as an oxidant, Ultrason. Sonochem., 15 (2008) 195–202.
[4] M. Roulia, Synthesis and characterization of novel chromium pillared clays, Mater. Chem. Phys., 91 (2005) 281–288.
[5] C. Ooka, H. Yoshida, M. Horio, K. Suzuki, T. Hattori, Adsorptive and photocatalytic performance of TiO_2 pillared mont-

morillonite in degradation of endocrine disruptors having different hydrophobicity, Appl. Catal., B 41 (2003) 313–321.
[6] R.L. Zhu, L.Z. Zhu, J.X. Zhu, F. Ge, T. Wang, Sorption of naphthalene and phosphate to the CTMAB–Al13 intercalated bentonites, J. Hazard. Mater., 168 (2009) 1590–1594.
[7] S.S. Gupta, K.G. Bhattacharyya, Adsorption of Ni (II) on clays, J. Colloid Interf. Sci., 295 (2006) 21–32.
[8] Y.S. Ho, G. McKay, Pseudo-second-order model for the sorption processes, Process Biochem., 34(5) (1999) 451–465.
[9] J.P. Chen, L. Wang, Characterization of metal adsorption kinetic properties in batch and fixed-bed reactors, Chemosphere, 54 (2004) 397–404.
[10] O. Keskinkan, M.Z.L. Goksu, A. Yuceer, M. Basibuyuk, C.F. Forster, Heavy metal adsorption characteristics of a submerged aquatic plant (Myriophyllum spicatum), Process Biochem., 39 (2003) 179–183.
[11] K.A. Matis, A.I. Zouboulis, N.K. Lazaridis, Removal and recovery of metals from dilute solutions: applications of flotation techniques, in: G.P. Gallios, K.A. Watis (Eds.), Mineral Processing and the Environment, Kluwer Academic Publishers, Dordrecht, The Netherlands., (1998) 165–196.
[12] T.J. Pinnavaia, Intercalated Clay Catalysts, Science, 220 (1983) 365–371.
[13] D. Wu, B. Zhang, C. Li, Z. Zhang, H. Kong, Simultaneous removal of ammonium and phosphate by zeolite synthesized from fly ash as influenced by salt treatment, J. Colloid Interf. Sci., 304 (2006) 300–306.
[14] H. Ye, F. Chen, Y. Sheng, G. Sheng, J. Fu, Adsorption of phosphate from aqueous solution onto modified palygorskites, Sep. Purif. Technol., 50 (2006) 283–290.
[15] J. Chen, H. Kong, D. Wu, X. Chen, D. Zhang, Z. Sun, Phosphate immobilization from aqueous solution by fly ashes in relation to their composition, J. Hazard. Mater., 139 (2007) 293–300.
[16] E. Oguz, Removal of phosphate from aqueous solution with blast furnace slag, J. Hazard. Mater., 114 (2004) 131–137.
[17] A.K. Golder, A.N. Samantha, S. Ray, Removal of phosphate from aqueous solutions using calcined metal hydroxides sludge waste generated from electrocoagulation, Sep. Purif. Technol., 52 (2006) 102–109.
[18] L. Zeng, X. Li, J. Liu, Adsorptive removal of phosphate from aqueous solutions using iron oxide tailings, Water Res., 38 (2004) 1318–1326.
[19] A. Genz, A. Kornmüller, M. Jekel, Advanced phosphorus removal from membrane filtrates by adsorption on activated aluminium oxide and granulated ferric hydroxide, Water Res., 38 (2004) 3523–3530.
[20] M.E. Roca Jalil, R. Vieira, D. Azevedo, M. Baschini, K. Sapag, Improvement in the adsorption of thiabendazole by using aluminum pillared clays, Appl. Clay Sci., 71 (2013) 55–63.
[21] A. Romero-Pérez, A. Infantes-Molina, A. Jiménez- Lòpez, E. Roca Jalil, K. Sapag, E. Rodriguez-Castellòn, Al-pillared montmorillonite as a support for catalysts based on ruthenium sulfide in HDS reactions, Catal., 187 (2012) 88–96.
[22] A. Khenifi, Z. Bouberka, K. Bentaleb, H. Hamani, Z. Derriche, Removal of 2, 4-DCP from wastewater by CTAB/bentonite using one-step and two-step methods: A comparative study, Chem. Eng. J., 146 (2009) 345–354.
[23] Li Gu, Jinli Xu, Lu Lv, Bing Liu, Huining Zhang, Xin Yu, Zhuanxi Luo, Dissolved organic nitrogen (DON) adsorption by using Al-pillared bentonite, Desalination, 269 (2011) 206–213.
[24] I. Ghorbel-Abid, K. Galai, M. Trabelsi-Ayadi, Retention of chromium (III) and cadmium (II) from aqueous solution by illitic clay as a low-cost adsorbent, Desalination, 256 (2010) 190–195.
[25] L.G. Yan, Y.Y. Xu, H.Q. Yu, X.D. Xin, Q. Wei, B. Du, Adsorption of phosphate from aqueous solution by hydroxy-aluminum, hydroxy-iron and hydroxy-iron–aluminum pillared bentonites, J. Hazard. Mater., 179 (2010) 244–250.
[26] S.M. Thomas, J.A. Bertrand, M.L. Occelli, F. Huggins, S.A. Gould, Microporous Montmorillonites Expanded with Alumina Clusters and M [(μ–OH) Cu (μ–OCH_2 CH_2NEt_2)]$_6$ $(ClO_4)_3$, (M = Al, Ga, and Fe), or Cr [(μ–OCH_3)$_3$ (μ–$OCH_2CH_2NEt_2$) $CuCl]_3$ Complexes, Inorg. Chem., 38 (1999) 2098–2105.
[27] A. Khenifi, Z. Bouberka, K. Bentaleb, H. Hamani, Z. Derriche, Removal of 2. 4–DCP from wastewater by CTAB/bentonite using one-step and two-step methods: A comparative study, Chem. Eng. J., 146 (2009) 345–354.
[28] L. Zhu, R. Zhu, Simultaneous sorption of organic compounds and phosphate to inorganic–organic bentonites from water, Sep. Purif. Technol., 54 (2007) 71–76.
[29] J.Q. Jiang, C. Cooper, S. Ouki, Comparison of modified montmorillonite adsorbents. Part I: Preparation, characterization and phenol adsorption, Chemosphere, 47 (2002) 711–716.
[30] E. Eren, B. Afsin, Y. Onal, Removal of lead ions by acid activated and manganeseoxide-coated bentonite, J. Hazard. Mater., 161 (2009) 677–685.
[31] J. Madejová, J. Budják, M. Janek, P. Komadel, Comparative FT-IR study of structural modifications during acid treatment of dioctahedral smectites and hectorite, Spectrochim., Acta, 54 (1998) 1397–1406.
[32] B. Tyagi, CD. Chudasama, RV. Jasra, Determination of structural modification in acid activated montmorillonite clay by FT-IR spectroscopy, Spectrochim. Acta, A, 64 (2006) 273–278.
[33] Y.S. Ho, Review of second-order models for adsorption systems, J. Hazard. Mater., 136 (2006) 681–689.
[34] I. Langmuir, The adsorption of gases on plane surfaces of glass, mica and platinum, J. Am. Chem. Soc., 40 (1918) 1362–1403.
[35] H.M.F. Freundlich, Over the adsorption in solution, Z. Phys. Chem., 57 (1906) 385–470.
[36] M.J. Temkin, V. Pyzhev, Recent modifications to Langmuir isotherms, Acta physiochim USSR., 12 (1940) 217–225.
[37] M.M. Dubinin, L.V. Radushkevich, The equation of the characteristic curve of activated charcoal, Dokl .Akad. Nauk Sssr., 55 (1947) 327–329.
[38] S.I. Lyubchik, A.I. Lyubchik, O.L. Galushko, L.P. Tikhonova, J. Vital, I.M. Fonseca, S.B. Lyubchik, Kinetics and thermodynamics of the Cr(III) adsorption on the activated carbon from co-mingled wastes, Colloids Surf., 242 (2004) 151–158.
[39] S.S. Tahir, N. Rauf, Thermodynamic studies of Ni(II) adsorption onto bentonite from aqueous solution, J. Chem. Thermodynam., 35 (2003) 2003–2009.
[40] V.K. Gupta, P. Singh, N. Rahman, Adsorption behavior of Hg (II), Pb(II), and Cd (II) from aqueous solution on Duolite C–433: a synthetic resin, J. Colloid Interf. Sci., 275 (2004) 398–402.
[41] A.A. Khan, R.P. Singh, Adsorption thermodynamics of carbofuran on Sn (IV) arsenosilicate in H^+, Na^+ and Ca^{2+} forms, Colloid Surf., 24 (1987) 33–42.
[42] A. Demirbas, A. Sari, O. Isildak, Adsorption thermodynamics of stearic acid onto bentonite, J. Hazard. Mater., B 135 (2006) 226–231.
[43] S. Kubilay, R. Gürkan, A. Savran, T. Sahan, Removal of Cu(II), Zn(II) and Co(II) ions from aqueous solutions by adsorption onto natural Bentonite, Adsorption, 13 (2007) 41–51.
[44] S. Babel, T.A. Kurniawan, Low-cost adsorbents for heavy metals uptake from contaminated water: a review, J. Hazard. Mater., 97 (2003) 219–243.
[45] E.I. Unuabonah, B.I. Olu-Owolabi, N.A. Oladoja, A.E. Ofomaja, L.Z. Yang, Pb/Ca ion exchange on kaolinite clay modified with phosphates, J. Soils Sediments, 10 (2010) 1103–1114.